

Analysis of Interleaved Arrays of Waveguide Elements

JAMES K. HSIAO

*Search Radar Branch
Radar Division*

April 16, 1971

PLEASE RETURN THIS COPY TO:

NAVAL RESEARCH LABORATORY
WASHINGTON, D.C. 20390
ATTN: CODE 2028

Because of our limited supply you are requested to return this copy as soon as it has served your purposes so that it may be made available to others for reference use. Your cooperation will be appreciated.

NDW-NRL - 5070/2035 (10-67)



NAVAL RESEARCH LABORATORY
Washington, D.C.

DOCUMENT CONTROL DATA - R & D

(Security classification of title, body of abstract and indexing annotation must be entered when the overall report is classified)

1. ORIGINAL ACTIVITY (Corporate author) Naval Research Laboratory Washington, D.C. 20390	
2a. REPORT SECURITY CLASSIFICATION Unclassified	2b. GROUP

3. REPORT TITLE
ANALYSIS OF INTERLEAVED ARRAYS OF WAVEGUIDE ELEMENTS

4. DESCRIPTIVE NOTES (Type of report and inclusive dates)
Interim report on a continuing NRL problem

5. AUTHOR(S) (First name, middle initial, last name)
James K. Hsiao

6. REPORT DATE
April 16, 1971

7a. TOTAL NO. OF PAGES
28

7b. NO. OF REFS
7

8a. CONTRACT OR GRANT NO.
NRL Problem R02-33

8b. PROJECT NO.
SR 11-141-005-13628

9a. ORIGINATOR'S REPORT NUMBER(S)
NRL Report 7248

9b. OTHER REPORT NO(S) (Any other numbers that may be assigned (this report))

10. DISTRIBUTION STATEMENT
Approved for public release; distribution unlimited.

11. SUPPLEMENTARY NOTES

12. SPONSORING MILITARY ACTIVITY
Department of the Navy (Naval Ship Systems Command), Washington, D.C. 20360

13. ABSTRACT
Multiple interleaved arrays of waveguide radiators have been analyzed at different frequencies. The approach is a generalization of the analysis of an infinite array at a single frequency. The presence of the low-frequency elements affects the radiation characteristics of the high-frequency elements and generates grating lobes which do not appear in a single-frequency array. Furthermore, power is coupled into the low-frequency waveguides when the high-frequency elements are excited. Numerical examples are presented which show that these effects are not severe. The analytical expressions reduce correctly to the single-frequency array case and satisfy the principle of energy conservation.

14. KEY WORDS	LINK A		LINK B		LINK C	
	ROLE	WT	ROLE	WT	ROLE	WT
Active admittance Antennas Arrays Multifrequency Waveguide radiators						

CONTENTS

	Page
Abstract	ii
Problem Status	ii
Authorization	ii
INTRODUCTION	1
DESCRIPTION OF THE PROBLEM	2
FORMULATION OF THE BOUNDARY VALUE PROBLEM	2
GRATING LOBES	7
POWER COUPLED AND ENERGY CONSERVATION	9
NUMERICAL RESULTS	9
SUMMARY	17
ACKNOWLEDGMENTS	17
REFERENCES	22
APPENDIX - Average Pattern	23

ABSTRACT

Multiple interleaved arrays of waveguide radiators have been analyzed at different frequencies. The approach is a generalization of the analysis of an infinite array at a single frequency. The presence of the low-frequency elements affects the radiation characteristics of the high-frequency elements and generates grating lobes which do not appear in a single-frequency array. Furthermore, power is coupled into the low-frequency waveguides when the high-frequency elements are excited. Numerical examples are presented which show that these effects are not severe. The analytical expressions reduce correctly to the single-frequency array case and satisfy the principle of energy conservation.

PROBLEM STATUS

This is an interim report on one phase of a continuing problem.

AUTHORIZATION

NRL Problem R02-33
Project SF 11-141-005-13628

Manuscript submitted January 13, 1971.

ANALYSIS OF INTERLEAVED ARRAYS OF WAVEGUIDE ELEMENTS

INTRODUCTION

A phased-array antenna, capable of operating in several frequency bands, may solve numerous problems encountered in shipboard and airborne radar systems. To obtain the best performance possible, the use of phased arrays is desirable in systems which perform several functions, such as surveillance, tracking, and guidance. Because each of these functions must be performed at optimum frequencies, several phased arrays are needed, each of which may require a sizable aperture. With the limited antenna space on ships and aircraft, this is quickly seen to be impractical. In the past, the problem of limited space has forced the use of a compromise frequency for multifunction radars and has resulted in degraded performance for some functions.

An ideal solution to this dilemma is a single-phased array capable of simultaneous operation at several widely spaced frequencies. Realization of such an array presents difficult engineering problems, whose solutions are not known at the present time. The next best approach, which appears more feasible, is the integration of several arrays, operating in different frequency bands, into a common aperture.

One approach to the design of such an array is shown in Fig. 1. Actually the aperture contains two arrays, one for a high-frequency band and the other for a low-frequency band. The waveguides are loaded with dielectric material to reduce their sizes, so that both arrays can be fitted into a single aperture. The purpose of this report is to show a method for computing the active admittance of such an array and also to analyze its radiation behavior.

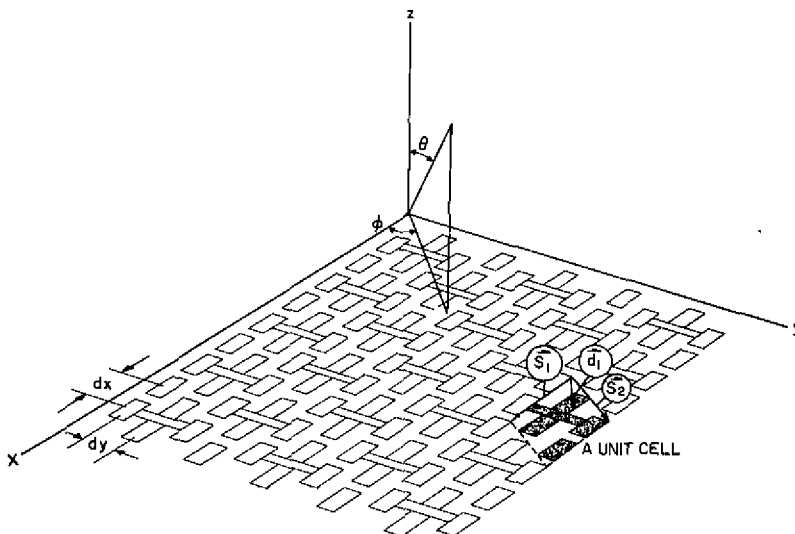


Fig. 1 - An interleaved array and the unit cell associated with it

Note: Part of this work has been reported in the 1970 G-AP International Symposium, September 14-16, 1970.

DESCRIPTION OF THE PROBLEM

One important feature of the interleaved array is that it is composed of a periodic structure and each period (henceforth called a unit cell) contains several different radiating elements. To simplify the analysis, this array is assumed to be infinite. The infinite array approach has been shown (1) to yield a reasonably accurate and simplified solution to the problem. Arrays of this nature have been treated previously (2-4). However, all of these studies are limited to the case in which each unit cell contains only a single element. The contribution of this report is then to extend the previous work to cover a more general case.

If the array is assumed to be infinite, field distributions in each unit cell are then identical; however, fields inside each waveguide in each unit cell are not necessarily identical. Therefore, the fundamental problem is to find the exact field distribution at each of these waveguides. Once this field is known, the active admittance of the excited mode and other pertinent parameters can then be determined. Since the fields in a waveguide are characterized by its modal functions, the problem is then to find the amplitude of each of these modal functions including both the propagating and evanescent modes. There are many approaches to this problem. The approach used here is the application of the concept of a transmission line (5). Since the fields are identical in each unit cell, each unit cell can be viewed as a transmission line with a discontinuity at the array face, but the transverse field must be continuous across this array face. Furthermore, the fields in the radiation region can be characterized by a set of modal functions as shown by Marcuvitz (6). Hence, by using this boundary condition and the known modal functions in both regions, a set of simultaneous equations can be formulated which can be used to solve for the amplitude of the modal functions either inside the waveguides or within the radiation region.

Several observations may be made about this array. First, since the array discussed here is a linear system, the response of this array to different frequencies can be solved separately by the superposition law. Second, the high-frequency waveguide is below cutoff when the array is operating at the low frequency; hence, these elements affect only the imaginary part of the radiation waves. Furthermore, no power can be coupled into these high-frequency elements. On the other hand, the low-frequency waveguides are considerably above the cutoff when the array is operating at the high frequency; therefore, some power may be coupled into these large waveguides. The amount of power coupled may be a function of the scan angle and the orientation of the waveguides. Moreover, the presence of these large waveguides may considerably change the radiation characteristics of the high-frequency elements. This change may also depend on the location of the high-frequency waveguides in relation to the low-frequency waveguide. The net result of this variation in radiation is to introduce a nonuniform illumination on the high-frequency array which may result in a high sidelobe (or grating-lobe) in the radiation pattern. All these problems will be explored in depth in the following sections.

FORMULATION OF THE BOUNDARY VALUE PROBLEM

Marcuvitz (6) has shown that the transverse field radiating into free space from a planar boundary can be characterized by a set of orthogonal modal functions:

$$\vec{\psi}^{TE} = \frac{1}{|\vec{k}_T|} (k_y \vec{a}_x - k_x \vec{a}_y) e^{j\vec{k}_T \cdot \vec{r}_T} \quad (1a)$$

$$\vec{\psi}^{TM} = \frac{1}{|\vec{k}_T|} (k_x \vec{a}_x + k_y \vec{a}_y) e^{j\vec{k}_T \cdot \vec{r}_T} \quad (1b)$$

where $\vec{\psi}^{TE}$ and $\vec{\psi}^{TM}$ are respectively the TE and TM modes,

$$\vec{k}_T = k_x \vec{a}_x + k_y \vec{a}_y, \quad (2a)$$

and

$$\vec{r}_T = x \vec{a}_x + y \vec{a}_y. \quad (2b)$$

A time-varying factor $e^{-j\omega t}$ is deleted for brevity.

The spectrum vector \vec{k}_T of the modal function is determined by the boundary conditions. In the present case, since the array is infinitely large, the field should repeat itself if the position vector \vec{r}_T progresses from one unit cell to another; hence,

$$\vec{k}_T \cdot \vec{S}_{mn} = 2\pi\ell, \quad (3)$$

where $\ell = 0, \pm 1, \pm 2 \dots$ and $\vec{S}_{mn} = m\vec{S}_1 + n\vec{S}_2$. (3a)

The terms \vec{S}_1 and \vec{S}_2 are the position vectors which describe a unit cell as shown in Fig. 1. In formulating Eq. (3), it is also assumed that \vec{S}_{00} has a zero phase reference. The term \vec{k}_T can be represented by two base vectors, as

$$\vec{k}_T = \vec{k}_1 + \vec{k}_2. \quad (4)$$

To satisfy Eq. (3), the following condition must be satisfied:

$$\vec{k}_i \cdot \vec{S}_j = 2\pi\delta_{ij}, \quad (5)$$

where

$$\delta_{ij} = 0, \text{ if } i \neq j$$

and

$$\delta_{ij} = 1, \text{ if } i = j.$$

In other words, \vec{k}_T is a reciprocal vector of vector \vec{S}_{mn} . Furthermore, for any $p, q = 0, \pm 1, \pm 2 \dots$, such that,

$$\vec{k}'_T(p, q) = p\vec{k}_1 + q\vec{k}_2, \quad (6)$$

Eq. (3) can also be satisfied. Therefore, the spectrum vector \vec{k}_T is characterized by two sets of integers, p and q . For waves radiated (or received) at an oblique angle (θ and ϕ) $\vec{k}'_T(p, q)$ becomes

$$\vec{k}_T(p, q, \theta, \phi) = \vec{k}'_T(p, q) \pm \vec{k}_\alpha, \quad (7)$$

where

$$\vec{k}_\alpha = k \sin\theta \cos\phi \vec{a}_x + k \sin\theta \sin\phi \vec{a}_y \quad (7a)$$

and

$$k = 2\pi/\lambda. \quad (7b)$$

In the following text, $\vec{k}'_T(p, q, \theta, \phi)$ will be shortened to \vec{k}_T . The propagation constant along

the z direction is related to this spectrum vector \vec{k}_T by

$$k_z(p, q, \theta, \phi) = \sqrt{k^2 - |\vec{k}_T|^2}. \quad (8)$$

This propagation constant k_z can be either real or imaginary depending on the mode of \vec{k}_T . The significance of the value of k_z is that it determines whether that mode is propagating or evanescent. To avoid grating lobes the spacing is usually adjusted between adjacent elements (equivalent to adjusting the unit cell dimensions) such that only one mode can be propagated in visible space. However, in the present case, where each unit cell contains more than one element, higher modes may propagate even though the spacings between adjacent elements are sufficiently small. This will be discussed further in a later section.

By defining the spectrum vector \vec{k}_T in this manner, the vector modal function $\vec{\Psi}$ becomes a set of orthogonal functions defined over a range of unit cell. Therefore, the transverse electric field in the radiation region can be represented as

$$\vec{E}_T(x, y, z) = \sum_R \sum_p \sum_q V_{pq}^R(z) \vec{\Psi}_{pq}^R(z), \quad (9a)$$

where R is used to represent the TE and TM modes. Similarly the magnetic field is then

$$\vec{H}_T(x, y, z) = \sum_R \sum_p \sum_q V_{pq}^R(z) y_{pq}^R \vec{a}_z \times \vec{\Psi}_{pq}^R(\vec{r}_T), \quad (9b)$$

where y_{pq}^R is the transmission line characteristic admittance of the (p, q) th mode, which is defined as

$$y_{pq}^{TM} = \frac{\omega \epsilon_0}{k_z(p, q, \theta, \phi)} \quad (10a)$$

and

$$y_{pq}^{TE} = \frac{k_z(p, q, \theta, \phi)}{\omega \mu_0}. \quad (10b)$$

The quantity $V_{pq}^R(z)$ which is the complex amplitude of the modal function, is a function of z . Since the $\vec{\Psi}_{pq}^R$ terms are orthogonal functions, the quantity $V_{pq}^R(z)$ can also be written as

$$V_{pq}^R(z) = \frac{1}{C} \iint_{cell} \vec{E}(x, y, z) \cdot (\vec{\Psi}_{pq}^R(\vec{r}_T))^* da. \quad (11)$$

The integration is performed over a unit cell and C is its area.

The transverse field inside the waveguides can be characterized by the waveguide modal functions. For example, the electrical field of the i th waveguide in the $(0, 0)$ th cell is

$$\vec{E}_i(x, y, z) = \sum_n V_{in}(z) \vec{\Phi}_{in}(\vec{r}_T + \vec{d}_i) e^{-j\vec{k}_a \cdot \vec{d}_i} e^{-j\vec{k}_a \cdot \vec{S}_{00}}. \quad (12)$$

The exponential factors $e^{-j\vec{k}_a \cdot \vec{d}_i}$ and $e^{-j\vec{k}_a \cdot S_{00}}$ are due to the progressive phase shift along the array face for beam steering. Vector \vec{k}_a is defined by Eq. (7a). The relative position of each waveguide within the unit cell should also be noted. Therefore, the vector modal function which is a function of the transverse coordinates must take into account this position difference between waveguides. Since the transverse E fields must be equal at the array face, $E(x, y, 0)$ from Eq. (11) can be replaced by the expression of Eq. (12), which gives

$$V_{pq}^R(0) = \frac{1}{C} \sum_i \iint_{a_i} \sum_n V_{in}(0) \vec{\Phi}_{in}(\vec{r}_T + \vec{d}_i) \cdot (\vec{\Psi}_{pq}^R(\vec{r}_T))^* da. \quad (13)$$

The integration over the unit cell is now partitioned and performed over each waveguide opening. If the order of summation and integration are changed and the coordinates of the integration are replaced with

$$\vec{r}'_T = \vec{r}_T + \vec{d}_i$$

and the relation of Eq. (7) is used, Eq. (13) can be manipulated into

$$V_{pq}^R(0) = \sum_i \sum_n V_{in}(0) \frac{1}{C} (C_{in, pq}^R)^* e^{j\vec{k}'_T(\rho, q) \cdot \vec{d}_i}, \quad (14)$$

where

$$(C_{in, pq}^R)^* = \iint \vec{\Phi}_{in}(\vec{r}'_T) \cdot (\vec{\Psi}_{pq}^R(\vec{r}'_T))^* da'$$

is the Fourier transform of the modal function $\vec{\Phi}_{in}$. Vector $\vec{k}'(\rho, q)$ is defined in Eq. (6).

The transverse magnetic field at the opening of the i th waveguide is

$$\vec{H}_i(x, y, 0^-) = \sum_n I_{in}(0) \vec{a}_z \times \vec{\Phi}_{in}(\vec{r}_T + \vec{d}_i) e^{-j\vec{k}_a \cdot \vec{d}_i} \quad (15a)$$

and

$$I_{in}(0) = \iint_{a_i} \vec{H}_i(x, y, 0^-) \cdot (\vec{a}_z \times \vec{\Phi}_{in}(\vec{r}_T + \vec{d}_i)) e^{-j\vec{k}_a \cdot \vec{d}_i} da \quad (15b)$$

due to the orthogonal property of the modal functions $\vec{\Phi}_{in}$, where

$$I_{in}(0) = \frac{a_{in} - R_{in}}{a_{in} + R_{in}} V_{in}(0) y_{in}. \quad (15c)$$

The quantities y_{in} , a_{in} , and R_{in} are respectively the characteristic admittance, the amplitude of the incident wave, and the amplitude of the reflected wave of the n th mode at the opening of the i th waveguide.

By invoking the boundary condition that the transverse magnetic field in both regions must be equal at the waveguide opening, and then following a procedure similar to the derivation of Eq. (14), Eq. (15) can be manipulated into

$$I_{in}(0) = \sum_R \sum_p \sum_q V_{pq}^R y_{pq}^R C_{in, pq}^R e^{-j\vec{k}_T^*(p, q) \cdot \vec{d}_i}, \quad (16)$$

where

$$C_{in, pq}^R = \iint_{A_i} \vec{\Phi}_{in}(\vec{r}_T) \vec{\Psi}_{pq}^R(\vec{r}_T) da.$$

The unknown quantities $V_{pq}^R(0)$ can be eliminated by replacing them with the relation of Eq. (13); then by changing the order of summation, the following expression results:

$$I_{in}(0) = \sum_j \sum_m V_{jm}(0) \sum_R \sum_p \sum_q y_{pq}^R \frac{1}{C} (C_{jm, pq}^R)^* (C_{in, pq}^R) \cdot e^{-j\vec{k}_T^*(p, q) \cdot (\vec{d}_i - \vec{d}_j)}. \quad (17)$$

Defining

$$y_{in, jm} = \sum_R \sum_p \sum_q y_{pq}^R \frac{1}{C} (C_{jm, pq}^R)^* (C_{in, pq}^R) \cdot e^{-j\vec{k}_T^*(p, q) \cdot (\vec{d}_i - \vec{d}_j)} \quad (17a)$$

and using the relation of Eq. (15c), Eq. (17) becomes

$$2a_{in} y_{in} = \sum_j \sum_m V_{jm} (y_{in, jm} + y_{in} \delta_{in, jm}), \quad (18)$$

where

$$\delta_{in, jm} = 0, \text{ if } i \neq j \text{ or } n \neq m,$$

and

$$\delta_{in, jm} = 1, \text{ if } i = j \text{ and } n = m.$$

Equation (18) can be expressed in a matrix form as

$$\begin{pmatrix} A_1 \\ A_2 \\ \vdots \\ A_I \end{pmatrix} = \begin{pmatrix} Y_{11} + y_1 Y_{12} & \cdots & Y_{1I} \\ Y_{21} & Y_{22} + y_2 & \cdots & Y_{2I} \\ \cdots & \cdots & \cdots & \cdots \\ Y_{I1} & \cdots & \cdots & Y_{II} + y_I \end{pmatrix} \cdot \begin{pmatrix} V_1 \\ V_2 \\ \vdots \\ V_I \end{pmatrix}. \quad (19)$$

I is the total number of waveguides in each unit cell. All the elements in this matrix are partitioned matrices, which are

$$\vec{A}_i = \begin{pmatrix} 2a_{i1} y_{i1} \\ 2a_{i2} y_{i2} \\ \vdots \\ 2a_{iN} y_{iN} \end{pmatrix}, \quad Y_{ij} = \begin{pmatrix} y_{i1, j1} & \cdots & y_{i1, jN} \\ y_{i2, j1} & \cdots & y_{i2, jN} \\ \cdots & \cdots & \cdots \\ y_{iN, j1} & \cdots & y_{iN, jN} \end{pmatrix},$$

$$V_i = \begin{vmatrix} V_{i1} \\ V_{i2} \\ \vdots \\ V_{iN} \end{vmatrix}, \text{ and } y_i = \begin{vmatrix} y_{i1} & 0 & \dots & 0 \\ 0 & y_{i2} & \dots & 0 \\ \dots & \dots & \dots & \dots \\ \dots & \dots & \dots & y_{iN} \end{vmatrix}.$$

N is the number of modes assumed to exist in each waveguide.

In the above expression, matrix $|A|$ represents the exciting function and matrix $|Y|$ is the scattering matrix in the sense that it relates the exciting function to the amplitude function $|V|$ of the waveguide modal function. Elements in the matrix $|Y|$ are the unknown quantities in this equation. Once these quantities are determined, it is a straightforward matter to find other pertinent parameters. Although this matrix equation seems to be very complicated, it can be solved easily on a fast digital computer.

The active admittance of the excited mode is given by

$$y_{in}^a = \frac{a_{in} - R_{in}}{a_{in} + R_{in}} y_{in}. \quad (20)$$

This active admittance is a very important parameter in the sense that it determines the element match in the active environment. The transmitted power of the excited mode can be found by

$$T_{in} = (a_{in} - R_{in})(a_{in} + R_{in}). \quad (21)$$

This is the power which actually radiates into free space. This radiated power can be further divided into three parts: one part will be radiated into the main beam, one part will be radiated into grating lobes, and the third part will be coupled into the low-frequency waveguides. In the following sections, these different components of power will be related to each other and will be determined quantitatively.

GRATING LOBES

The radiation pattern of an infinite array is essentially an impulse function having an infinitesimally narrow beam in visible space. This corresponds to the situation in which only one of the radiation wave modes is propagating in the z direction. In general this propagating mode is the TEM mode ($p=0, q=0$). This situation, generally, can be achieved by adjusting the dimensions of the unit cell. For a single-frequency array, each unit cell contains only one element. Hence, vectors \vec{S}_1 and \vec{S}_2 also represent the spacing between adjacent elements. Therefore, if the spacing between elements is kept sufficiently small, grating lobes can always be avoided. However, each unit cell of a multiple-frequency array contains more than one element. Controlling element spacing in this array type does not necessarily suppress the grating lobes. This can be best illustrated in the case where an array is steered to broadside. For this case, $\vec{k}_z = 0$. According to Eq. (8), the following conditions must be maintained to avoid a grating lobe in a multiple-frequency array:

$$|\vec{k}_1| \geq k, \text{ for } p = 1, q = 0, \quad (22)$$

and

$$|\vec{k}_2| \geq k, \text{ for } p = 0, q = 1.$$

For a single-frequency array, the following relations apply:

$$\vec{K}_1 \cdot \vec{s}_1 = 2\pi, \vec{K}_2 \cdot \vec{s}_2 = 2\pi, \quad (23)$$

where \vec{s}_1 and \vec{s}_2 are the spacings between adjacent elements. Now assume that a multiple-frequency array has an identical lattice structure to that of a single-frequency array, and let there be I and J elements respectively in the \vec{s}_1 and \vec{s}_2 directions in each unit cell. Then the unit-cell dimension vectors \vec{S}_1 and \vec{S}_2 are related to the vectors \vec{s}_1 and \vec{s}_2 by

$$\vec{S}_1 = I\vec{s}_1, \vec{S}_2 = J\vec{s}_2. \quad (24)$$

The relation in Eq. (23) leads to

$$I\vec{k}_1 = \vec{K}_1, J\vec{k}_2 = \vec{K}_2. \quad (25)$$

Inserting Eq. (25) into Eq. (22) gives

$$|I\vec{k}_1| \geq k, |J\vec{k}_2| \geq k. \quad (26)$$

Equation (26) indicates that in a multiple-frequency array for modes with $p < I$ or $q < J$, the propagation constant $k_z(p, q, \theta, \phi)$ might be real; hence, grating lobes may exist.

For an array of the configuration shown in Fig. 1, the position of the high-frequency elements can be represented by

$$\vec{d}_i = u \frac{\vec{S}_1}{I} + v \frac{\vec{S}_2}{J}, \quad (27)$$

where

$$u = 0, 1, 2, \dots, I - 1,$$

$$v = 0, 1, 2, \dots, J - 1,$$

and

$$\vec{k}_T'(p, q) \cdot \vec{d}_i = p \frac{u}{I} 2\pi + q \frac{v}{J} 2\pi. \quad (28)$$

Inserting these relations into Eq. (13) gives the amplitude of the high-order mode ($p, q \neq 0$) as

$$V_{pq}^R = \sum_{i(u, v)} \sum_n V_{in}(0) (C_{in}^R)^* e^{j(p \frac{u}{I} + q \frac{v}{J}) 2\pi} + \sum_k \sum_\ell V_{k\ell} (C_{k\ell, pq}^R)^* e^{j\vec{k}_T'(p, q) \cdot \vec{d}_k}. \quad (29)$$

The summations of indices k and ℓ in the last term are for the low-frequency elements. Now assuming that these low-frequency elements do not exist, V_{in} and $C_{in, pq}^R$ become identical for all the high-frequency elements, and $V_{pq}^R = 0$, if p and q are not respectively integer multiples of I and J . This shows that if the size of a unit cell is arbitrarily chosen some of the high-order modes may fictitiously exist but their amplitudes are zero, which is analogous to the situation of representing a periodic function by a Fourier series. The period may be arbitrarily chosen to be an integer multiple of the actual period. But the frequency components which are not integer multiples of the fundamental frequency would vanish.

From this, it may be concluded that the existence of the grating lobes is due to the difference of the amplitudes of the modal functions among the high-frequency waveguides and the nonvanishing amplitudes of the modal functions in the low-frequency waveguides.

POWER COUPLED AND ENERGY CONSERVATION

Amitay and Galindo (7) have shown that the mathematical formulation of the waveguide phased-array problem retains the energy conservation properties. The total power radiated from each unit cell, from the relation of the Poynting vector, is

$$P_r = \iint_{\text{cell}} \vec{E}_T(x, y, 0^+) \times [\vec{H}_T(x, y, 0^+)]^* \cdot \vec{a}_z \, da, \quad (30a)$$

while the power transmitted from each waveguide to the array face per unit cell is

$$P_w = \sum_i \iint_{a_i} \vec{E}_i(x, y, 0^-) \times [\vec{H}_i(x, y, 0^-)]^* \cdot \vec{a}_z \, da. \quad (30b)$$

Since the transverse fields must be continuous across the array face,

$$P_r = P_w. \quad (31)$$

This expression includes both the real power and the imaginary power.

If the E and H fields in Eq. (30a) are replaced by Eqs. (9a) and (9b), and those in Eq. (30b) by Eqs. (12) and (15a), the relation of equation (31) becomes

$$C \sum_R \sum_p \sum_q |V_{pq}^R|^2 y_{pq}^R = \sum_i \sum_n V_{in} I_{in}^*. \quad (32)$$

The real part on the left side of Eq. (32) consists of those terms which have a real y_{pq}^R . These usually include the (0,0) mode and possibly high-order modes. The (0,0) mode term is the power radiated into the main beam and high-order modes are power radiated into the grating lobes. The real part of the right side of this equation can be divided into two parts. One part is the power transmitted from the waveguides which are excited, and the other part is the power coupled into the unexcited waveguides. By equating the real parts and using the index i to represent the excited waveguides and the index k for the unexcited waveguides Eq. (32) can be rearranged into

$$\sum_i \sum_n (|a_{in}|^2 - |R_{in}|^2) = C \sum_R |V_{00}^R|^2 y_{00}^R + C \sum_R \sum_p \sum_q |V_{pq}^R|^2 y_{pq}^R + \sum_k \sum_\ell |V_{k\ell}|^2 y_{k\ell}. \quad (33)$$

The summation term on the left side of this equation is the power fed into each unit cell. The first term on the right side is the power radiated into the main beam and the second term represents the power radiated into the grating lobes. The third term represents the power coupled into the propagating modes of the unexcited waveguides. Thus, the amount of power coupled into the low-frequency waveguides and the level of the grating lobes can be quantitatively determined from Eq. (33).

NUMERICAL RESULTS

The matrix in Eq. (19) was coded into a computer program in Fortran language and then computed on the CDC 3800 at NRL. To check the correctness of this program, a few

examples of single-frequency arrays (wherein each unit cell contains only one element) with known data were computed and then compared. Further checks, such as energy conservation (7), were also performed. Although this method does not examine the accuracy of the numerical solution, it does, however, check the correctness of the computational process.

The number of modes which should be used in both the waveguide region and the radiation region have been discussed extensively in the literature (3, 4) for the case of a single-frequency array. However, so far no criterion is available which may be used to choose the right modes to obtain a certain given accuracy. Naturally, use of as many modes as possible is desirable, but, on the other hand, the computation time may become astronomically lengthy. A thousand modes in the radiation region have been used. Subsequently, when the number is reduced to about 500, the difference is not more than 1 percent. Also, the dimensions of the unit cell have been enlarged several times as compared with those of a single-frequency array. As pointed out earlier in this report, the spectrum vector $\vec{k}'_{r(p,q)}$ is the reciprocal of the unit-cell dimension vector. Therefore, it would be anticipated that more modes are needed to achieve a given accuracy than are required for a single-frequency array.

The number of modes which should be used in the waveguide, as pointed out by earlier workers (3), need be only three or four of the lowest-order modes to yield a reasonably accurate solution. However, in the present case attention should be directed to the modes which are propagating in the low-frequency waveguides, since these represent a power loss. Furthermore, because of the different orientation and size of the low-frequency waveguide, it is not necessary that the lowest-order mode in this waveguide have the largest amplitude. Therefore, choosing only a few low-order modes may give erroneous results. In a later example, it will be shown that the amplitudes of modes inside the low-frequency waveguide vary widely for different planes of scan. Eight to nine modes have been used. Later it was learned that only three or four of these modes have significant amplitudes, although they are different for different planes of scan. The error remains very small, if the right modes are chosen.

Four cases have been studied. All of them are arrays of rectangular waveguides, loaded with dielectric material. Two of them have a triangular grid structure; while the other two have a rectangular grid structure. For convenience in comparing results, the waveguide dimensions and the elements spacings are kept constant in all four cases. Each unit cell, in all these cases, contains four high-frequency elements and one low-frequency element. This gives an operating frequency ratio of 2:1 between the high-frequency array and the low-frequency array with the same scan coverage. For the purpose of investigating the effect of power coupling into the low-frequency waveguide, this waveguide is intentionally enlarged. It has dimensions, in terms of the wavelength of the high frequency of $a = 0.7545\lambda$ and $b = 0.1994\lambda$ and is loaded with material of a relative dielectric constant $\epsilon_r = 9$. The high-frequency elements have the dimensions $a = 0.3956\lambda$ and $b = 0.1575\lambda$ and are loaded with a dielectric material with $\epsilon_r = 4$. In both the rectangular grid case and the triangular grid case, the low-frequency waveguides were oriented in two different ways with respect to the high-frequency elements, either perpendicular or parallel to them. Moreover, the low-frequency waveguide is always located in the center of the unit cell and is symmetrically spaced with respect to the four high-frequency elements, except in the case of the triangular grid with perpendicularly-oriented low-frequency elements, where the center element is located slightly nonsymmetrically.

The case in which the low-frequency elements were excited was computed. However, the radiation characteristics were essentially the same as those of single-frequency array. Furthermore, no power is coupled into the high-frequency elements, since they are below cutoff and no grating lobe will exist due to the effect of enlarging the unit cell. In other words, the presence of the high-frequency elements does not seem to affect appreciably the operation of the low-frequency array. Therefore, the computed results are not presented here.

In the following presentations, only the high-frequency elements are assumed to be excited, and the excitation is limited to the dominant mode (TE_{10}) only.

Figures 2 and 3 show respectively the computed results of a triangular grid array with the low-frequency elements perpendicular to the parallel to the high-frequency elements. Figures 2a and 3a show the transmission characteristics of the four high-frequency elements vs scan angle in the three planes of scan ($\phi = 0^\circ, 45^\circ, \text{ and } 90^\circ$). The basic patterns are similar to those of a single-frequency array, except that the four curves (one for each element) are spread apart. This spreading characteristic is a function of the scan angle and also of the relative position of the high-frequency element. However, this nonuniformity of radiation does not seem to be severe. Notice that a resonant point exists at $\theta = 68^\circ$ in the $\phi = 45^\circ$ plane of scan, which is actually a grating lobe point of the high-frequency array.

These patterns were compared with the one computed for a single-frequency array. The transmission coefficient for the single-frequency array was found to be approximately equal to the average of those for the four elements in a unit cell of the dual-frequency array. To explore this effect, an analysis is presented in the Appendix, which indicates that this formulation does indeed degenerate into the case of a single-frequency array. Furthermore, if the amplitudes of the low-frequency waveguide modal functions are very small, the average pattern of the high-frequency elements in each unit cell is closely similar to that of a single-frequency array. This is what our computer results showed.

The amounts of power coupled into the idling low-frequency waveguides for the perpendicular case and the parallel case are shown respectively in Figs. 2b and 3b. This is the total power coupled, which includes all propagating modes in the low-frequency waveguides, in percent of the radiated power. For illustration, the contributions of each mode at a particular scan angle are listed in Table 1. It can be seen from this table that only a few modes make a significant contribution. Furthermore, they are different in different scan planes. Judging from Figs. 2b and 3b, the total power coupled into the low-frequency waveguide is less than 10 percent of the total radiated power within the usable scan range. Furthermore, the coupled power stays rather constant in the usable scan range. At the grating lobe point (at $\theta = 68^\circ$ in the $\phi = 45^\circ$) a large amount of power is coupled into the low-frequency waveguide. Also, in the parallel case a sort of resonance phenomenon occurs at $\theta = 35^\circ$ in the H-plane scan. It is of interest to notice that at this particular angle of scan a grating lobe occurs in the rectangular grid array with the same dx and dy spacings.

Figures 2c and 3c show the maximum grating lobe level vs scan angle in the three planes of scan. The level of this grating lobe in general is less than -20dB in both the perpendicular and parallel cases. The shapes of these curves are similar, although in the parallel case they exhibit an oscillatory nature.

It is concluded from Eq. (29) that these grating lobes are due to the nonuniformity of the amplitudes of the modal functions among the high-frequency elements within a unit cell and also due to the nonvanishing amplitudes of the modal functions in the low-frequency elements. The former effect is equivalent to having the array nonuniformly, periodically illuminated. It is well known that this in general introduces a high sidelobe level. The second effect is due to the spacing of the low-frequency elements too large to suppress the grating lobes.

Figures 2d and 3d show respectively the total power distributions for the perpendicular and parallel cases. The top curves show the total power radiated into the main beam and the bottom curves represent the total losses, which include both the power coupled into the low-frequency waveguide and the power loss into the grating lobes. These values are plotted as a percent of the total radiated power. According to the principle of conservation of energy (7), the sum of these components should be unity. It can

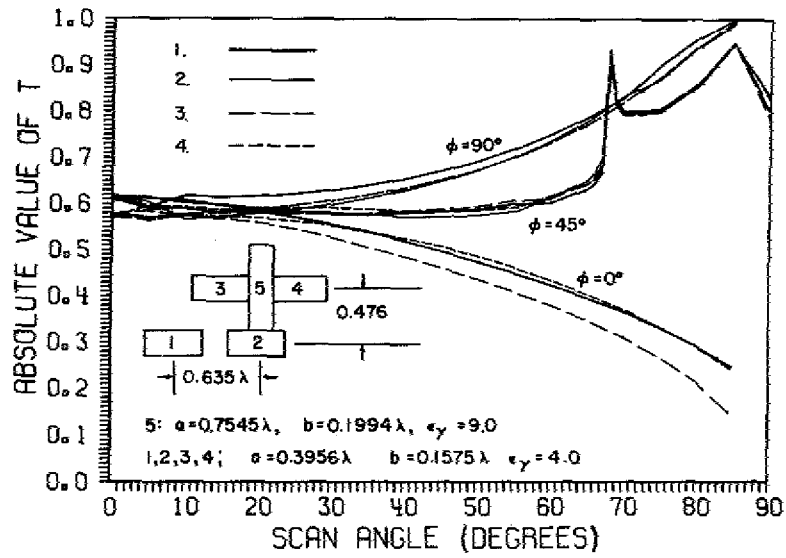


Fig. 2a - Transmission coefficient vs scan angle for the triangular grid, perpendicular case

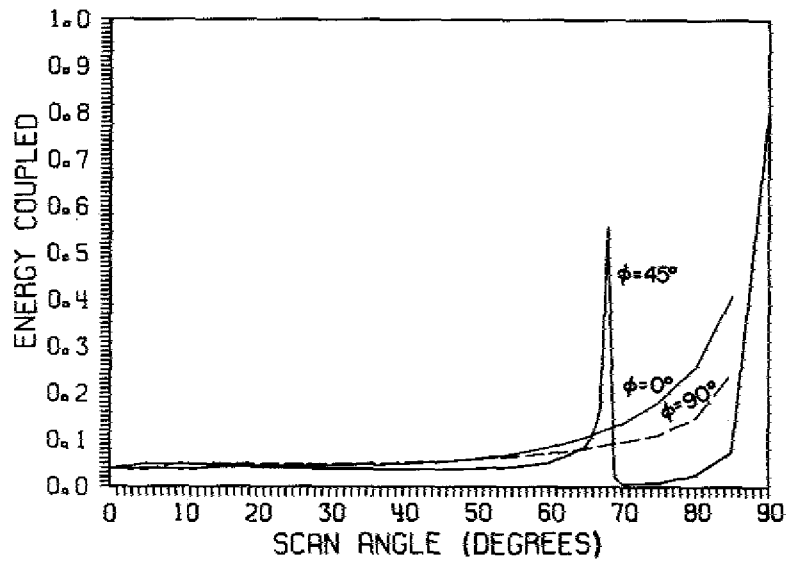


Fig. 2b - Energy coupled into low-frequency waveguide for the triangular grid, perpendicular case

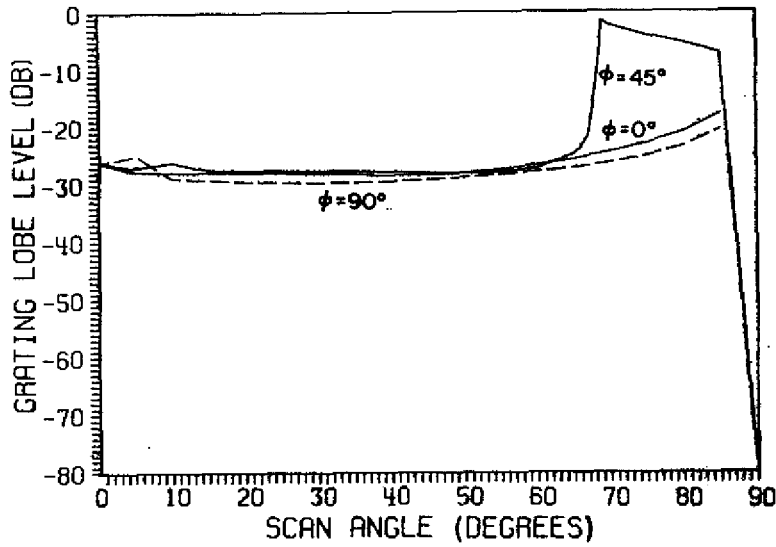


Fig. 2c - Maximum grating lobe level for the triangular grid, perpendicular case

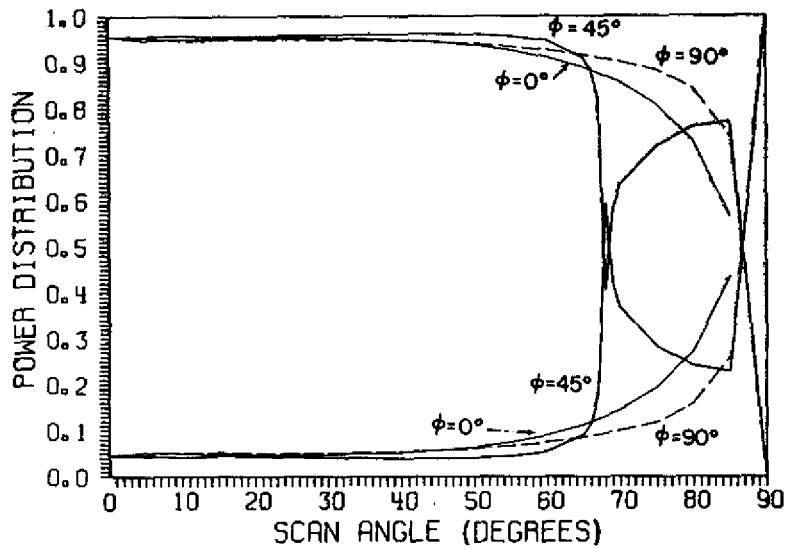


Fig. 2d - Power distribution for the triangular grid, perpendicular case (upper curves represent power radiated into main beam; lower curves represent total loss)

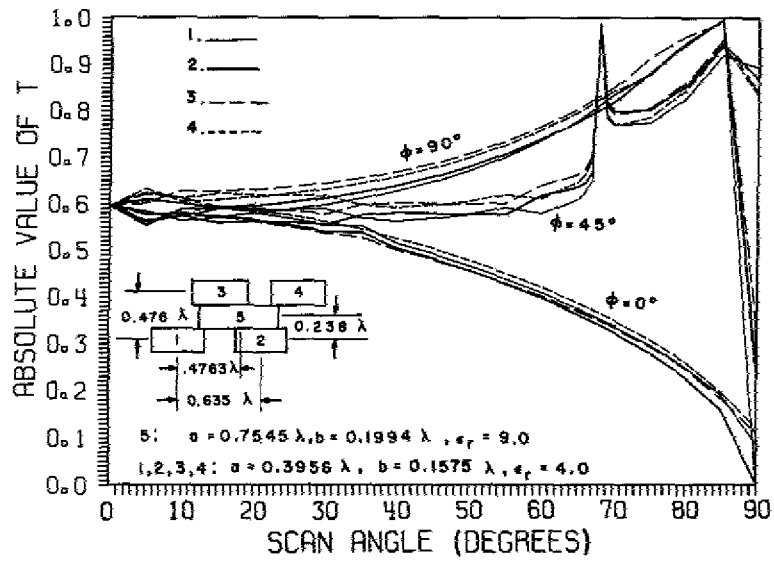


Fig. 3a - Transmission coefficients vs scan angle for the triangular grid, parallel case

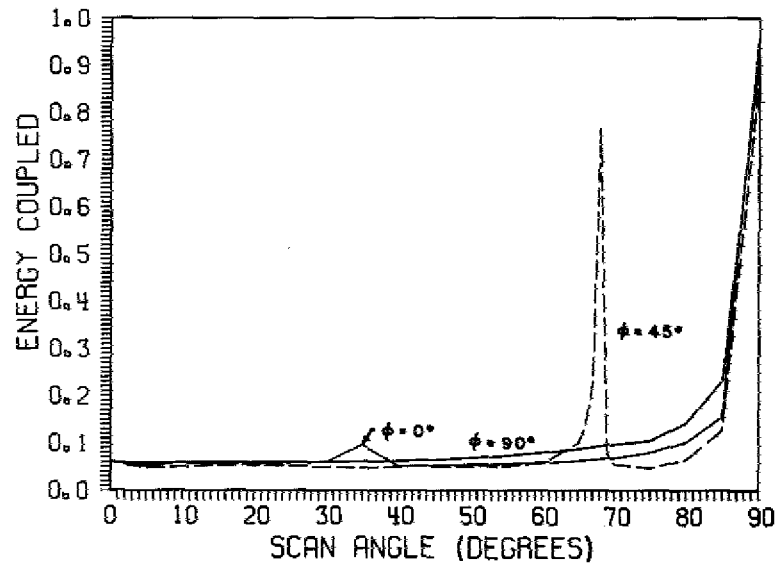


Fig. 3b - Energy coupled into the low-frequency waveguide for the triangular grid, parallel case

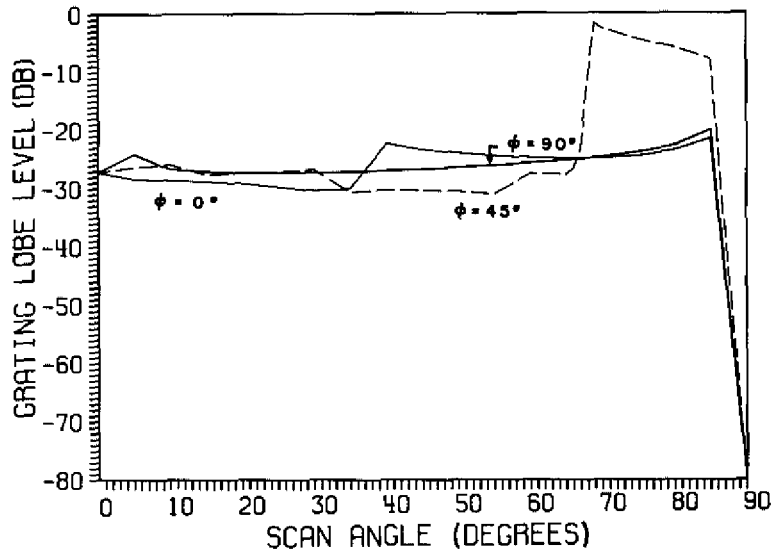


Fig. 3c - Maximum grating lobe level for the triangular grid, parallel case

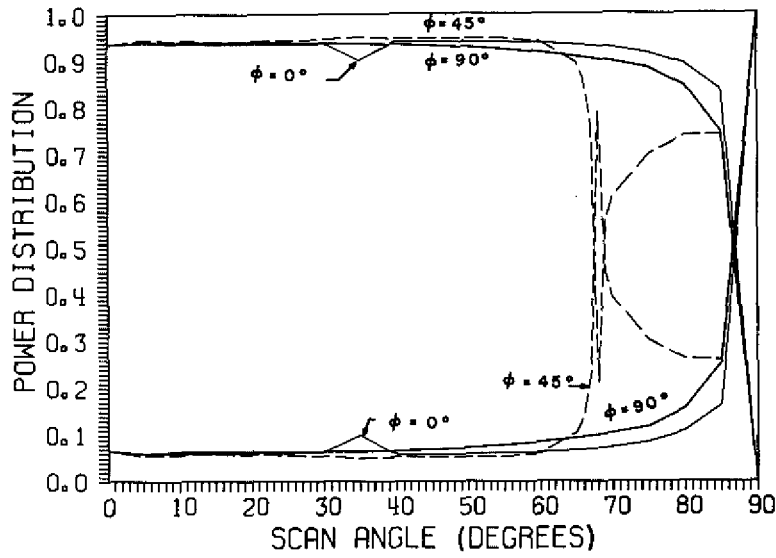


Fig. 3d - Power distribution for the triangular grid, parallel case (upper curves represent power radiated into main beam; lower curves represent total loss)

Table 1
Power Coupled Into Low-Frequency Waveguide:
Triangular Grid Array

Plane	TE ₁₀	TE ₂₀	TE ₃₀	TE ₄₀	TE ₀₁	TE ₁₁	TE ₂₁	TM ₁₁
Perpendicular Case Modes								
$\theta = 0^\circ$	0.0221	0.0000	0.0033	0.0000	0.0120	0.0000	0.0054	0.0000
H-plane $\theta = 24^\circ$	0.0000	0.0012	0.0000	0.0006	0.0382	0.0000	0.0050	0.0000
D-plane $\theta = 24^\circ$	0.0271	0.0044	0.0022	0.0009	0.0105	0.0003	0.0025	0.0002
E-plane $\theta = 24^\circ$	0.0000	0.0000	0.0000	0.0000	0.0354	0.0111	0.0018	0.0004
Parallel Case Modes								
$\theta = 0^\circ$	0.0375	0.0000	0.0054	0.0000	0.0018	0.0000	0.0189	0.0000
H-plane $\theta = 24^\circ$	0.0295	0.0093	0.0018	0.0010	0.0000	0.0137	0.0170	0.0002
D-plane $\theta = 24^\circ$	0.0338	0.0040	0.0031	0.0011	0.0005	0.0048	0.0153	0.0002
E-plane $\theta = 24^\circ$	0.0370	0.0020	0.0047	0.0002	0.0008	0.0001	0.0108	0.0004

be seen from these figures that this is indeed the case. In general, more than 90 percent of the total power is radiated into the main beam and less than 10 percent appears in the "loss" components. Furthermore, comparing Figs. (2d) and (3d) with Figs. (2b) and (3b), most of these losses are seen to be due to the power coupled into the low-frequency waveguides. Less than 1 percent of the loss actually is radiated into the grating lobes.

The computed results for the rectangular grid array including both perpendicular and parallel cases are shown in Figs. (4) and (5). In general, they are very similar to those for the triangular case. The spacing of the grid structure of the high-frequency array results in a grating lobe at $\theta = 35^\circ$ in the H-plane scan. However, in contrast to the triangular case, the power coupled into the low-frequency waveguide does not exhibit a resonance phenomenon at this grating lobe point. Furthermore, with scan beyond this point, the power radiated into the grating lobe (true) increases steadily. Beyond $\theta = 50^\circ$, more power is radiated into the grating lobe than into the main beam. However, in the triangular grid case, the grating lobe level is always less than that of the main beam.

SUMMARY

1. A method has been derived to solve the boundary value problem of an array which may consist of many different waveguide radiating elements interleaved into a single array.

2. The presence of the low-frequency waveguides affects the radiation characteristics of the high-frequency elements. Furthermore, because the low-frequency waveguides operate above cutoff, power will be coupled into them when the high-frequency elements are excited.

3. Due to the nonuniformity of the amplitude of the modal functions in the high-frequency waveguides and the nonvanishing amplitudes of the modal functions in the low-frequency waveguides, grating lobes appear in visible space even though the spacing of the high-frequency array is sufficiently small to suppress the grating lobes.

4. A method has been shown for computing the power coupled into the low-frequency waveguides and the level of the grating lobes.

5. Computed results of four different interleaved arrays have been shown. In these examples, the interleaved array really consists of two arrays, one for the high-frequency and the other for the low-frequency. The grating lobe level due to the presence of the low-frequency waveguides is less than -20dB while the power coupled into the low-frequency waveguides is less than 10 percent of the total radiated power.

6. The formulation derived has been demonstrated to degenerate correctly into a single-frequency array case, which is considered to justify the correctness of this approach. This approach also retains the energy conservation properties.

ACKNOWLEDGMENTS

Comments from R. J. Adams, S. K. Meads, R. M. Brown, and discussions with V. Galindo are hereby gratefully acknowledged.

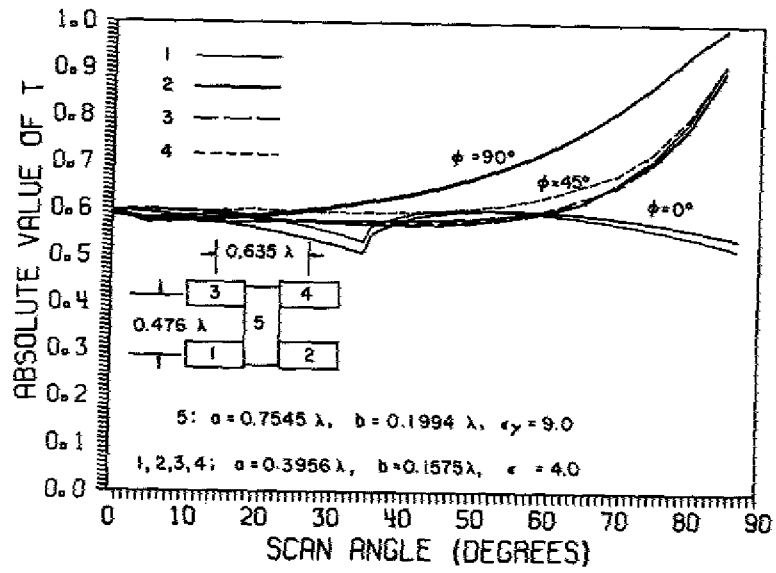


Fig. 4a - Transmission coefficient vs scan angle for the rectangular grid, perpendicular case

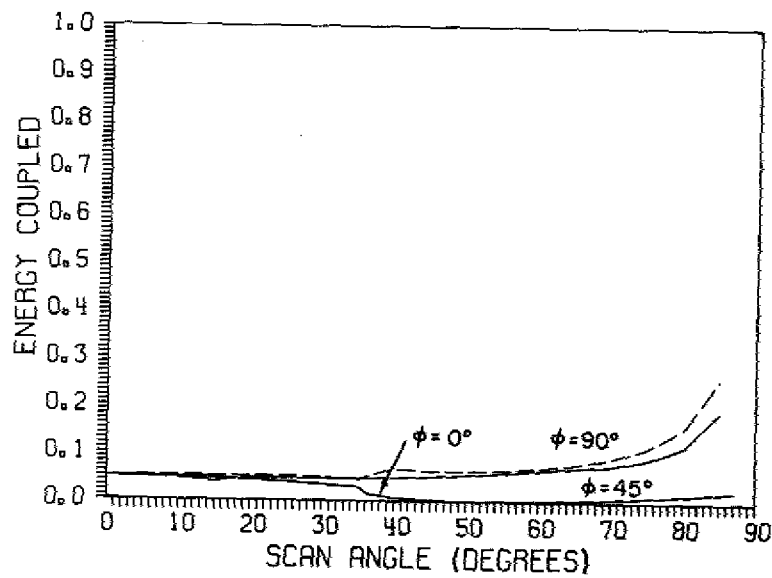


Fig. 4b - Energy coupled into low-frequency waveguide for the rectangular grid, perpendicular case

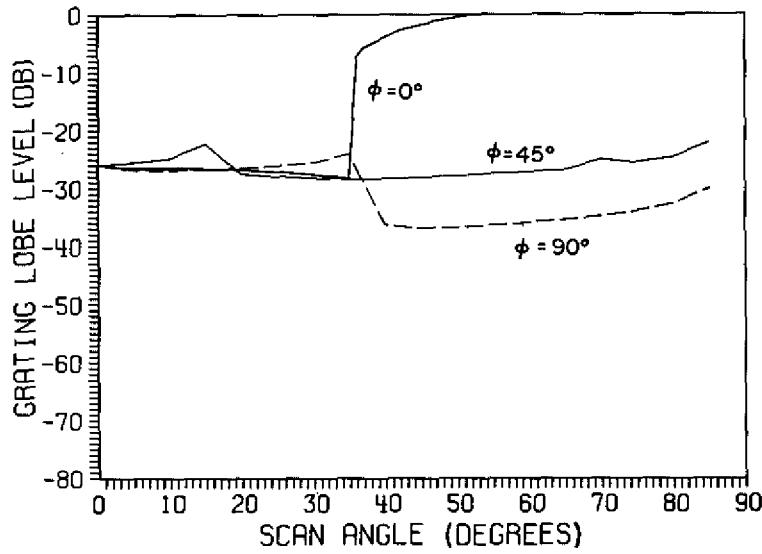


Fig. 4c - Maximum grating lobe level for the rectangular grid, perpendicular case

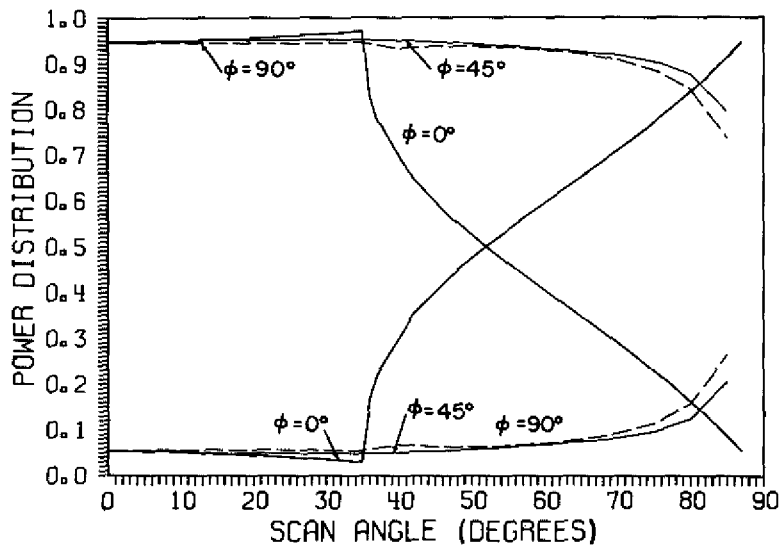


Fig. 4d - Power distribution for the rectangular grid, perpendicular case (upper curves represent power radiated into main beam, lower curves represent total loss)

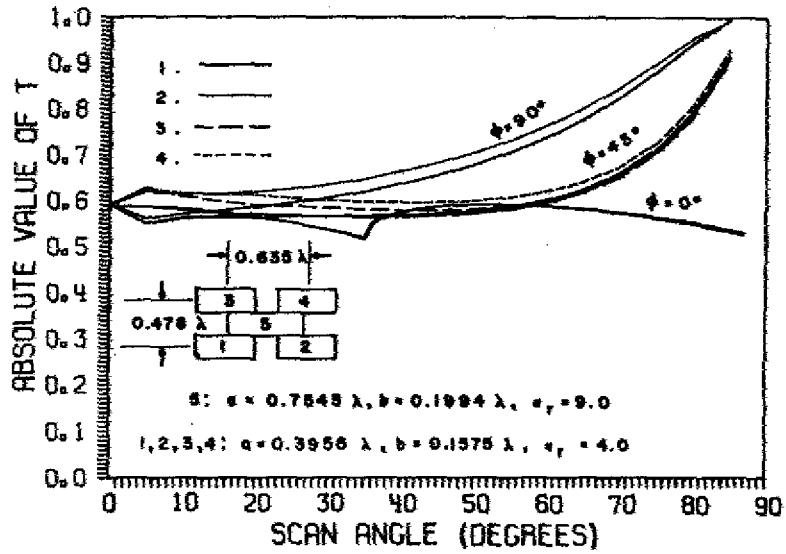


Fig. 5a - Transmission coefficient vs scan angle for the rectangular grid, parallel case

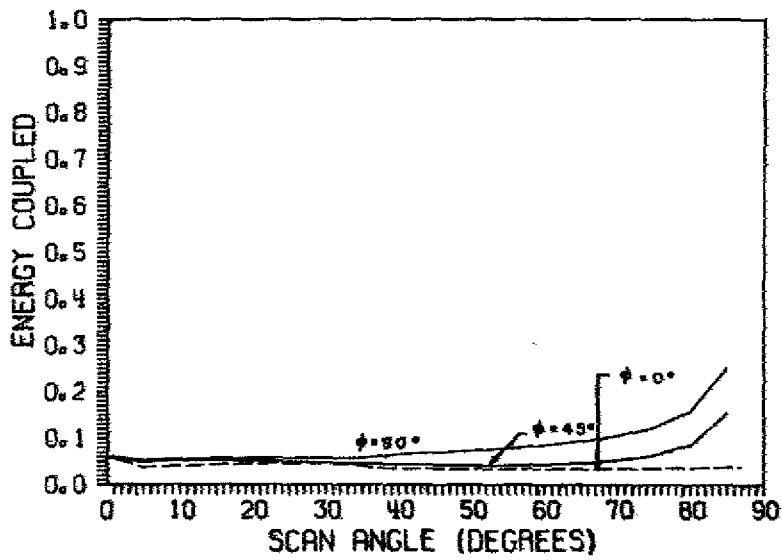


Fig. 5b - Energy coupled into low-frequency waveguides for the rectangular grid, parallel case

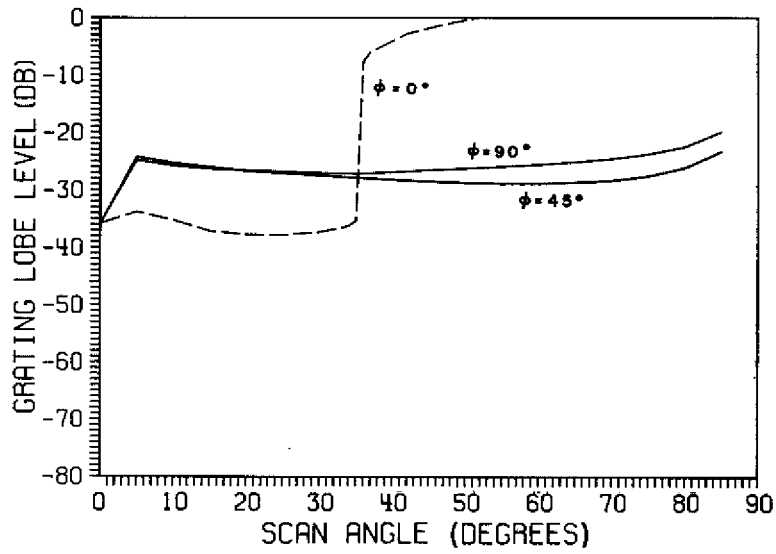


Fig. 5c - Maximum grating lobe level for the rectangular grid, parallel case

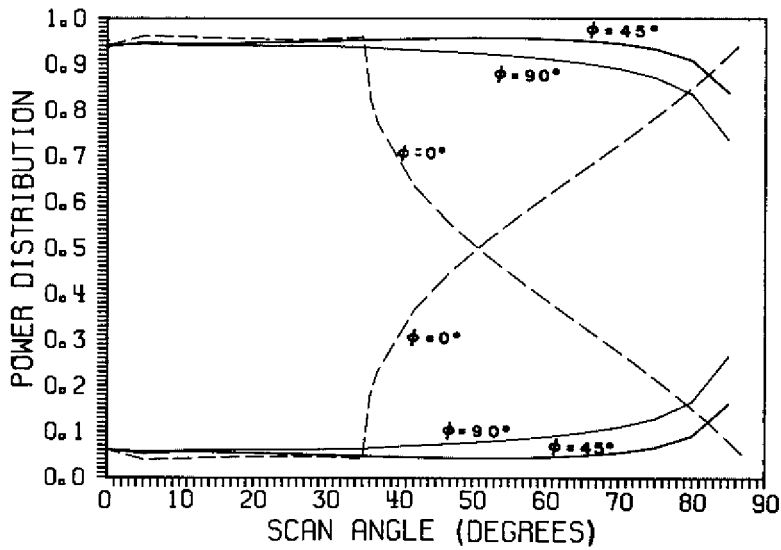


Fig. 5d - Power distribution for the rectangular grid, parallel case (upper curves represent power radiated into main beam, lower curves represent total loss)

REFERENCES

1. Hansen, R. C. , editor, "Microwave Scanning Antennas, " Vol. 2, New York: Academic Press, 1966.
2. Galindo, V. , and Wu, C. P. , "Numerical Solutions for an Infinite Phased Array of Rectangular Waveguides with Thick Walls, " IEEE Trans. Antennas and Propagation AP-14 (No. 2): 149 (1966).
3. Borgiotti, G. V. , "Modal Analysis of Periodic Planar Phased Arrays of Apertures, " Proc. IEEE 56 (No. 11): 1881 (1968).
4. Diamond, B. L. , "A Generalized Approach to the Analysis of Infinite Planar Array Antennas, " Proc. IEEE 56 (No. 11): 1837 (1968).
5. Marcuvitz, N. , and Schwinger, J. , "On the Representation of the Electric and Magnetic Fields Produced by Currents and Discontinuities in Wave Guides. I, " J. Appl. Phys. 22 (No. 6: 806 (1951).
6. Marcuvitz, N. , editor, "Waveguide Handbook, " M. I. T. Radiation Laboratory Series, Vol. 10, New York: McGraw-Hill, 1951.
7. Amitay, N. , and Galindo, V. , "On Energy Conservation and the Method of Moments in Scattering Problems, " IEEE Trans. Antennas and Propagation AP-17 (No. 6): 747 (1969).

APPENDIX

AVERAGE PATTERN

From Eq. (18), the expression derived for the n th excited mode in the i th waveguide is

$$2a_{in}y_{in} = \sum_j \sum_m V_{jm} (y_{in,jm} + y_{in}\delta_{in,jm}) + \sum_k \sum_\ell V_{k\ell} y_{in,k\ell}.$$

In this equation the terms due to the high-frequency elements and the low-frequency elements have been separated. Indices j and m represent the m th mode in the j th high-frequency element; indices k and ℓ represent the ℓ th mode in the k th low-frequency waveguide. If all the equations involving the n th mode of all the high-frequency waveguides are summed, the following equation results:

$$2 \sum_i a_{in}y_{in} = \sum_j \sum_m V_{jm} \sum_i y_{in,jm} + y_n \sum_i V_{in} + \sum_k \sum_\ell V_{k\ell} \sum_i y_{in,k\ell}, \quad (A1)$$

where

$$\sum_i y_{in,jm} = \frac{1}{C} \sum_R \sum_p \sum_q y_{pq}^R (C_{jm,pq}^R)^* \cdot \sum_i (C_{in,pq}^R) e^{j\vec{k}'_T(p,q) \cdot (\vec{d}_j - \vec{d}_i)}. \quad (A2)$$

Notice that the order of the summation in the above equation is changed. Assume that all high-frequency waveguides are identical and that there are a total of I elements in the \vec{S}_1 direction and J elements in the \vec{S}_2 direction in each unit cell. Then those terms in the above equation whose indices are not respectively integer multiples of I and J , by the relation of Eq. (28a), become zero, giving the equation

$$\sum_i y_{in,jm} = \frac{1}{C} L \sum_R \sum_p \sum_q y_{pq}^R (C_{jm,pq}^R)^* (C_{in,pq}^R) \quad (A3a)$$

for the high-frequency elements, where L is the total number of high-frequency elements in each unit cell. For the low-frequency elements

$$\sum_i y_{in,k\ell} = \frac{1}{C} L \sum_R \sum_p \sum_q y_{pq}^R (C_{k\ell,pq}^R)^* (C_{in,pq}^R) e^{j\vec{k}'_T(p,q) \cdot \vec{d}_k}. \quad (A3b)$$

If each high-frequency element has an identical excitation, Eq. (A2) then becomes

$$2a_n y_n = \sum_m \bar{V}_m y_{n,m} + y_n \bar{V}_n + \sum_k \sum_\ell V_{k\ell} y_{n,k\ell}, \quad (A4)$$

where

$$y_{n,m} = \frac{1}{C'} \sum_R \sum_p \sum_q y_{pq}^R (C_{m,pq}^R)^* (C_{n,pq}^R)$$

and

$$y_{n,k\ell} = \frac{1}{C} \sum_R \sum_p \sum_q y_{pq}^R (C_{k\ell,pq}^R)^* (C_{n,pq}^R) e^{j\vec{k}'_T(p,q) \cdot \vec{d}_k}$$

The summation of the series is performed only on those indices p and q which are respectively integer multiples of I and J . Here

$$C' = C/L$$

is the area of a unit cell of the high-frequency array, and

$$\bar{v}_n = \frac{1}{L} \sum_I v_{in}$$

is the average amplitude of the n th mode of the high-frequency elements in each unit cell. If the last summation in Eq. (A4) is neglected, this equation becomes identical to the equations that are used for the characterization of a single-frequency array. If the low-frequency waveguides were short-circuited, the amplitudes of the modal functions $v_{k\ell}$ in these waveguides would vanish. This is equivalent to the effect of covering the low-frequency waveguides with a ground plane, and the array then becomes essentially a single-frequency array. From this it may be concluded that the formulation presented here indeed degenerates into the case of a single-frequency array, which may indicate the validity of this approach.